RSC Advances

ROYAL SOCIETY OF CHEMISTRY

www.rsc.org/advances

The influence of putrescine on the Structure, Enzyme Activity and stability of α-Chymotrypsin

Sadegh Farhadian[a], Behzad Shareghi [a*] , Ali A. Saboury [b,c], Mina Evini [b]

[a] Department of Biology, Faculty of Science, University of Shahrekord, Shahrekord, P. O. Box.115, Iran.

[b] Institute of Biochemistry and Biophysics, University of Tehran, Tehran, Iran.

[c] Center of Excellence in Biothermodynamics, University of Tehran, Tehran, Iran

[*] Corresponding author: Tel.: +989131093764, fax: +983832324419,

E-mail address: b_shareghi@yahoo.com

Abstract

Information on protein stability is essential to study protein structure, activity, and interactions with ligands. The interaction of putrescine with α-Chymotrypsin (α-Chy) was investigated by using different types of spectroscopic techniques in an aqueous medium at two temperatures of 25 and 35°C, in combination with a molecular docking study and molecular dynamic simulation. Fluorescence measurements showed that the observed quenching was a dynamic one. The intrinsic fluorescence of α-Chymotrypsin was decreased in the presence of putrescine due to the excited-state proton transfer. Additionally, Circular dichroism results revealed that putrescine binding had no dramatic influence on the α-Chymotrypsin structure. Molecular docking also indicated that the hydrogen bonds interactions dominated in the binding site.

Keywords: α-Chymotrypsin, putrescine, Fluorescence, Circular dichroism, Molecular Docking.

1. Introduction

Proteins are of utmost importance to cellular function, and they need to be and remain properly folded to perform their function. Information on the protein stability is essential to study protein folding, structure, activity, and interactions with ligands[1]. The specificity and precision of protein stability have enthralled chemists and biochemists from the very beginning of modern biochemistry and protein science, turning it to one of the most rapidly advancing fields nowadays. The quantitative description of the forces that govern the formation of protein folding is a part of this attempt. The native structure of proteins corresponds to a structure that is thermodynamically stable under physiological conditions.

Protein stability and associations depend on the electrostatic, hydrophobic, van der Waals, and steric interactions with themselves and with solvent molecules[2]. All approaches to understanding the molecular basis of protein stability ultimately depend on reliable experimental determinations of the thermodynamics of protein unfolding for the protein structure[3]. Thermodynamic folding properties such as the Gibbs free energy of unfolding (ΔG_u), enthalpy change (ΔH), heat capacity change (ΔC_p) and transition temperature (T_m) values for the enzyme or proteins are in hand, helping us to predict these parameters by molecular dynamic simulation and molecular docking studies.

The stability of native proteins changes marginally in an organic compound environment and can dramatically affect the proteins' functional activities. Polyamines [putrescine (PUT), $NH_2(CH_2)_4NH_2$; spermidine, and spermine] are essential for cell growth. Natural polyamines are fully protonated at the physiological pH. Due to their cationic nature, they interact with negatively charged molecules including nucleic acids, phospholipids and proteins[4,5]. In relation to the interaction of polyamines with proteins, the importance of negatively charged, polar and aromatic residues has been confirmed. Polyamines are small cationic molecules

which can bind by electrostatic interactions to various macromolecules such as proteins and nucleic acids[4,6]. Thus, not only is the charge pattern of a polyamine relevant in its interaction with biomolecules, but also the hydrophobic polymethylene backbone which confers structural flexibility and the possibility of secondary binding interactions may play a determining role [7]. The protein surface primarily interacts with the surrounding solvent that contributes to its folding/unfolding. Thus, the properties of the enzyme surface may be important for maintaining its catalytic active conformation in non-natural environments. Enzymes are widely used as catalysts in nonconventional media because they offer a number of advantages in such media[8].

It is well known that enzymes are mild, highly specific and efficient biocatalysts in a wide range of applications[9]. α-Chymotrypsin (α-Chy) is a serine protease with three chains connected by five disulfide bonds. This enzyme is a globular β protein with 245 amino acids and a secondary structure dominant in an anti-parallel β-sheet with some small α-helix content that has a catalytic activity in the hydrolysis of ingested proteins in the intestine[9, 10]. This protein is folded into two anti-parallel β-barrel domains consisting of a Greek key motif followed by an anti-parallel hairpin one[11].

The purpose of the present study was to investigate the interactions of α-Chy with polyamines such as putrescine in order to determine thermodynamic parameters of the binding and the nature of interactions. Various spectroscopic techniques including UV-Vis spectroscopy, fluorescence spectroscopy and circular dichroism (CD), as well as molecular docking and molecular dynamic simulation, were used to this end.

2. Materials and methods

2.1. Materials

α-Chymotrypsin, putrescine dihydrochloride and *N*-benzoyl-l-tyrosyl-ethyl ester (BTEE) were purchased from Sigma and used without further purification. All α-Chy solutions were prepared at the pH 8. All solutions were made in a 50 mM Tris-HCl buffer (pH 8.0). When required, the pH of putrescine stocks was readjusted to one of 8.0.

2.2 Methods

2.2.1 Thermal stability of α-Chy

The thermal stability of free protein and protein-putrescine complexes was investigated by monitoring absorbance intensities at different temperatures. The UV–Vis spectrum of α-Chy at 280 nm was obtained with UV–Visible spectrophotometer in the presence and absence of various amounts of putrescine. The system was first baselined with Tris-HCl buffer and then α-Chy spectra were obtained upon the titration of putrescine. All studies were carried out in quartz cells including 0.1 mg/cm^3 α-Chy and different concentrations of putrescine. The scan rate was 0.1 ºC/min at 280 nm for the solutions of α-Chy (0.1mg/ml) in the presence and absence of the putrescine. The absorption data were plotted as a function of temperature. The melting temperature, T_m, which was defined as the temperature in which ΔG^o was zero, was determined as the transition midpoint of the melting curve.

2.2.2. *Enzymatic activity assay*

The catalytic activity of 25 μg/ml α-Chy (E.C. 3.4.21.1; type II from bovine pancreas, Sigma) was determined by UV-Vis spectrophotometer at 256 nm and 37 ºC by the rate of BTEE (N-Benzoyl-l-Tyrosine Ethyl Ester; Sigma) hydrolysis in 50 mM Tris/HCl, with the pH of 8, and in the absence and presence of 0 - 0.5 mM putrescine for the steady-state kinetics. The K_m for α-Chy was determined at 37 ºC by measuring the steady-state activity of the enzyme, with

BTEE ranging from 0.1 to 0.5 mM in the absence and presence of 0, 0.1, 0.3 or 0.5 mM putrescine.

2.2.3 UV–Vis absorption spectra

The UV–visible absorption spectra were measured using an Ultrospec 4000 Pharmacia UV–Vis Spectrophotometer equipped with a thermostatic cell holder. The concentration of α-Chy was 0.1 mg/ml. The system was baselined with Tris-HCl buffer and then α-Chy spectra were obtained upon the titration of putrescine. The absorbance changes were recorded at 280nm. All studies were carried out in quartz cells containing 0.1 mg/ml α-Chy and different concentrations of putrescine solution. The resulting absorbance changes in the presence and absence of putrescine were plotted versus putrescine concentration.

2.2.4 Fluorescence Spectroscopy Measurements

Fluorescence spectroscopy studies were performed using a Shimadzu RF-5301 fluorescence spectrophotometer equipped with a temperature adjustable cell holder. The emission spectrum was measured from 290 to 450 nm in the presence and absence of different concentrations of putrescine and at the temperatures of 25 and 35 °C, with the excitation wavelength being at 280 nm and 295 nm. The slits were 3 nm for excitation and 5 nm for emission scans. The fluorescence spectra were recorded in each step of temperature elevating processes. The solution was secured for 4 min before the scan to equilibrate the sample solution fully. Fluorescence of α-Chy was excited with some monochromated light of 280 nm generated by a xenon arc lamp. Fluorescence spectra were recorded over the range of 290–450 nm. Measurements were carried out on the systems of α-Chy-putrescine-buffer as a function of temperature. In addition, the buffer was collected as backgrounds in the same temperature region. At each temperature, the samples were thermally equilibrated for at least 4 min before measurement; after this time, no time-dependence of the fluorescence spectra was detected.

All studies were carried out in quartz cells containing 2 cm^3 (0.1 mg/ml) α-Chy and different concentrations of putrescine solution.

2.2.5. Circular dichroism

Circular dichroism (CD) spectra in the far-UV (190–260 nm) and near-UV (260–320 nm) regions were obtained by an AVIV 215 spectropolarimeter at 25 ºC, using a 1 mm-path cell for far-UV and a 10 mm-path cell for near-UV experiments. Protein concentration was 8 μM (0.2 mg/ml) and 16 μM (0.4 mg/ml), respectively, in the absence and presence of various concentrations of polyamine. The spectra were recorded after 4 min incubation with putrescine to allow sample equilibration as stated above. Protein secondary structure was determined by the CDNN program, version 2.1.0.223, using a network trained with 33 complex spectra as the reference set[4]. Based on a mean amino acid residue weight (MRW) of 98.5Da for α-Chy with a molecular weight of 25 kDa, the CD results were given in molar ellipticity [θ] (deg cm^2 mol^{-1}). According to statistical methods implemented in the CD software of CDNN, secondary structure changes of α-Chy were determined in the absence and presence of various concentrations of putrescine.

2.2.6. Molecular Docking Studies

In this study, we employed AutoDock software (Version 4.2, available at http://autodock.scripps.edu) to perform molecular docking. The AutoDock is an automated docking program designed for the prediction of the binding among small molecules such as substrates or drug candidates and the receptor with a known 3D structure[12]. This program is designed to predict how small molecules, such as drug candidates, bind to a receptor. For the ligand conformational searches, the Lamarckian genetic algorithm (LGA) was selected. To perform the molecular docking between α-Chy and putrescine, we employed the α-Chy structures (PDB code: 1YPH) which were solved at the resolutions of 1.34° A[13]. RCSB

Protein Data Bank was employed too (available at http://www.rcsb.org). Putrescine molecular structure was modeled using HyperChem 8.0.6 program and optimized to minimal energy using Gaussian 98 program[14]. All nonpolar hydrogens were merged and partial atomic charges were assigned using the Gasteiger-Marsili method. Different grid boxes with different grid points in size and the grid-point spacing of 0.375 Å were considered for docking. Each map was centered such that it covered the entire protein, including all possible binding sites. The generated ligand was docked into the defined binding site on the α-Chy structure. Ligplot plus was used to analyze the docking poses for H-bond and hydrophobic interactions.

2.2.7 Molecular dynamic simulation

The lowest free-binding energy conformation of α-Chy was selected as the initial conformation for the molecular dynamics (MD) studies. MDS was performed by GROMACS 5.4.7 package and G43a1 force field[15]. In the first step, the topology and interaction parameters were generated using the GROMOS96 43a1 force field[16], with the intermolecular potential represented as a sum of Lennard-Jones (LJ) force and pairwise Coulomb interaction. Long-range electrostatic force was also determined by the particle mesh Ewald (PME) method[17]. The calculations were carried out using the structure of the putrescine components and α-Chy was downloaded from the Protein Data Bank. The proteins and ligands were located in a cubic box with SPC water model, along with the specifications of boxes and the number of water ions. Although more complex water models are nowadays frequently used in the simulation of proteins, we chose to use the SPC as it was found to give superior results for the simulations of solutes in water when compared to more sophisticated water models, especially at the interfaces. The box volume, which was 1 $nm^{3,}$ was filled with extended simple-point charge (SPC) water molecules and the solvated systems were neutralized by adding 40 Na^+ and Cl^- ions. Corresponding to a salt concentration of ~140 mM, these ions

were added to the system by replacing the water molecules in random positions. Energy minimization was performed using the steepest descent method for the 4000 time-step. Next, the system was equilibrated for 20 ps at a temperature of 300 K. Finally, a 10 ns MD simulation was carried out at 0.1 MPa and 300 K. A 10-ns-long production MD run was performed after the equilibration. During the MD run, the LINCS algorithm[18] was used to constrain the lengths of hydrogen-containing bonds; the waters were restrained using the SETTLE algorithm[19]. The time step for the simulation was 2 fs. The simulations were run under NPT conditions, using Berendsen's coupling algorithm[20], to keep the temperature and the pressure constant (P = 1 bar, τP = 0.5 ps; T = 300 K; t = 0.1 ps). Van der Waals forces were treated using a cutoff of 12 Å. Long-range electrostatic forces were treated using the particle mesh Ewald method[17]. The coordinates were saved every 0.5 ps.

3. Results and Discussion

3. 1 Thermal stability of α-Chy

The net stability of a protein is defined as the difference in the free energy (ΔGº) between the native (folded) and denatured (unfolded) states[25]. We can represent the equilibrium between these two states using a simple mechanism shown below:

$$F \text{ (folded)} \leftrightarrow U \text{ (unfolded)}$$

And define the net protein stability as shown in Eq. (1) [25, 26]:

$$\Delta G^{o} = G_U - G_F = -PT \ln K = -RT \ln \frac{[U]}{[F]} \qquad \text{Eq. (1)}$$

,where [U] and [F] and G_U and G_F denote the concentrations and the free energies of the unfolded and folded states, respectively. K is the equilibrium constant[27]. The thermodynamic parameters, standard free energy (ΔG°), and T_m were estimated to appraise the feasibility and the exothermic nature of the adsorption process. The fraction of the unfolded form, F_U, was computed by normalizing denaturation curves and utilizing the following Eq. (2):

$$F_u = \frac{(Y-Y_F)}{Y_U-Y_F} \qquad \text{Eq. (2)}$$

In this equation, Y shows the observed variable parameter at a given denaturant concentration. Y_F and Y_U are the variable characteristics of the folded and unfolded states, respectively; also, these values were acquired by the linear extrapolation of pre- and post-transition regions[28]. The resulting changes in F_U, in the presence and absence of Putrescine particle, were plotted versus temperature (Fig. 2).

The equilibrium constant, K_U, was computed by utilizing the values of F_U. The computation of K_U values between the folded and unfolded states of protein at a given denaturant concentration could be done by Eq. (3):

$$K_u = \frac{F_u}{1-F_u} = \frac{Y_f-Y}{Y-Y_u} \qquad \text{Eq. (3)}$$

Gibbs free-energy changes (ΔG^{o}_{U}) were computed from K_D values using Eq. (4):

$$\Delta G^{\circ}{}_u = -RTlnK_u = -RTln\left[\frac{F_u}{1-F_u}\right] = -RTln[\frac{Y_f-Y}{Y-Y_u}] \qquad \text{Eq. (4)}$$

In this equation, R is the gas constant (1.987 cal/deg/mol) and T is the absolute temperature[29]**.** The Gibbs free-energy of unfolding, ΔG^{o}_{U}, as a function of temperature for α-Chy in the presence and absence of putrescine, is shown in Fig. 3. These results could be used to determine T_m at which ΔG^{o}_{U} =0. Our results also suggested that by increasing putrescine concentrations, the curves were shifted to the upper temperatures (Fig. 3). α-Chy T_m at variable concentrations of putrescine can be seen in Table 1. As indicated in Table 1, by increasing putrescine concentrations, T_m of α-Chy was increased.

3.3. Absorption spectroscopy

UV–vis absorption measurement is a very convenient technique to display the structural change of a protein and obtain information regarding the protein–ligand complex formation. Therefore, this study investigated the effect of polyamines such as putrescine concentration on

the absorption spectrum of α-Chy. The UV–vis absorption spectra of α-Chy in the absence and presence of a definite concentration of putrescine are shown in Fig. 1. There were main absorption peaks at 260–300 nm [21, 22]. It could be seen that by increasing the concentration of putrescine, the absorbance was increased. The results showed that the addition of putrescine to the solution of the α-Chy caused a slight hyperchromic effect at 280 nm. The slight increase in the absorbance of α-Chy showed that the structure of α-Chy had small variation after binding to the putrescine. The results proved that the binding between putrescine and α-Chy had no remarkable effect on the protein skeleton structure[22-24].

3. 3. Circular dichroism spectra

3.3.1 Far-UV CD

Far CD spectroscopy is one of the most widely utilized techniques for detecting the secondary structure changes of proteins when interacting with ligands, thereby making it possible to quantify conformational modifications in the 3D structure[22]. The analysis of far-UV CD spectra (190–260 nm) could be used to assess the content of different secondary structure elements in proteins. The CD spectrum of α-Chy in buffer had a minimum at ≈202−205 nm (depending on the pH value) and no positive band[30, 31]. By using it, the fractions contents of different secondary structures of α-Chy in the absence and presence of putrescine were calculated using the software package CDNN. Details of fraction changes have been listed in Table 2. The far-UV CD spectra of α-Chy and α-Chy - putrescine mixture are shown in Fig 4. α-Chy was folded into two domains with very little α-helix content and extensive regions of anti-parallel β-sheets, along with two interchain and three intrachain disulphide bonds[32]. Spectral deconvolution of α-Chy spectrum in the buffer showed 11.9% of α- helix, 20.5% of β structures, 27.7% of turns and 40% of the unordered structure. The data proposed that the secondary structure change and the unfolding of the protein skeleton by putrescine were low.

The conformational changes here implied that the exposure of some hydrophobic regions previously buried was increased, and that putrescine bound the amino acid residues of the main polypeptide chain of the protein and destroyed their hydrogen bonding networks[33].

All the experiments above provided good evidence showing that the conformational change of α-Chy was caused by the interaction between putrescine and the protein.

3.3.2. Near-UV CD

In order to assure that the observed effects were related to conformational changes, near-UV CD (240–320 nm wavelengths) was also used. In this technique, the spectrum of a protein is essentially a contribution of Tyr and Trp residues and disulphide bonds that can be affected by the flexibility and the number of aromatic side chains. This technique can be very useful to study changes by external factors on the resulting tertiary structures [34]. The near-UV CD spectra of the enzyme indicated that the α-Chy had a particular tertiary structure in each of the solvents with different concentrations of putrescine.

The near-UV CD spectrum of α-Chy (Fig.5) in the buffer display the contributions of Tyr and Trp residues responsible for peaks and shoulders between 270 and 305 nm, and those of Phe residues which strongly contribute to bands in the 258–270 nm region[35]. Therefore, the disappearance of these bands suggested the enhanced flexibility of peptide chains around aromatic residues due to a partial unfolding of the proteins. The CD spectrum in the near-UV region was very complicated, since the microenvironment for each amino acid in a protein was different. Nevertheless, the asymmetry of the microenvironments was lost when a protein was unfolded, and the corresponding decrease in the near-UV CD signals reflected the degree of tertiary structure loss around the aromatic chromophores[31].

The results of α-Chy structure in putrescine showed that the maxima at 280-300 nm could be best assigned to Trp residues. The intensity of this band was decreased when the

aromatic residues were away from each other, that is, the native structure of the protein was not preserved in the putrescine solution. The ellipticity values in the near UV-CD region were changed with a decrease in the peak intensity in the presence of putrescine. When putrescine was added to the solution of the α-Chy, a gradual negative decline in the molar ellipticity values was observed. This difference in ellipticity could be attributed to the unfolding of the α-Chy. Therefore, these changes suggested the enhanced flexibility of peptide chain around aromatic residues due to the partial unfolding of α-Chy. The analysis of near CD results has been displayed in Fig. 5. As can be seen, α-Chy showed the change in the tertiary structure at 0.1-0.3 mM concentration of putrescine. After 5 min of incubation with putrescine, changes occurred in the 270–305 nm regions, thereby indicating a conformational change that led to a more flexible environment near the aromatic residues.

The CD spectrum of α-Chy in the 250–300 nm region was a composite of disulphide nσ*, tyrosyl L_b and tryptophanyl L_a and L_b contributions. The L_b transition was extremely sensitive; however, the L_a transition was less sensitive to conformational changes. This spectral region was dominated by the contribution of the aromatic residues (e.g. Trp and Tyr) and disulphide bridges, while the intensity of the 250–300 nm bands was affected by local conformational changes around these chromatophores. The major bands of Trp were located in the 300 nm region and those of Tyr around 280 nm regions. The bands of Phe were usually weaker than those of the other two residues and often escaped detection around the 260 nm region[3]. The intrinsic fluorescence only monitored the changes in some of the Trp residues, while the near-UV CD had the contributions of all aromatic residues, not only tryptophans[35]. It is reasonable to assume that the spectral changes observed by intrinsic fluorescence, UV–vis and near-UV CD were related to the changes in α-Chy conformation upon binding to putrescine.

3.4 The effect of putrescine concentration on fluorescence quenching

Fluorescence spectroscopy is a useful technique to study tertiary structure transitions, the denaturation process, and dynamic, thermodynamic and ligand binding parameters in proteins with fluorophore residues (e.g. Trp, Tyr, or Phe), because the intrinsic fluorescence of these residues is particularly sensitive to the polarity of microenvironments along the transition[36]. In this method, changes can occur in the maximal intensity of fluorescence and the red-shift of the maximal emission wavelength [22]. The intrinsic fluorescence of tryptophan residues is used because of the intensity of emission and the high sensitivity of tryptophan fluorophore to the changes in the polarity of its microenvironments[36-38]. Fluorescence of α-Chy originates from tryptophan (Trp), tyrosine (Tyr) and phenylalanine (Phe) residues. α-Chy is a globular protein containing eight tryptophan residues, and its intrinsic fluorescence is almost contributed by the Trp residues. Trp172, Trp207 (46%), Trp215, and Trp237 (49%) are completely exposed to the solvent[3, 35, 39]. The latter three residues are situated in direct proximity to the active site residues. Trp5l and Trpl41 are completely buried in the globule core, and Trp27 and Trp29 are partly exposed to the solvent. The intrinsic fluorescence of α-Chy is mainly contributed by the tryptophan residue alone, because the phenylalanine residue has a very low quantum yield and the fluorescence of tyrosine is almost totally quenched when it is ionized or when it is near an amino group, a carboxyl group, or a tryptophan[9, 40]. The change in the intrinsic fluorescence intensity of α-Chy is mainly due to the Trp residue when small molecules are bound to α-Chy. Additionally, the changes in the emission spectra from Trp are also related to the protein conformational transitions, subunit association apart from anion binding, or direct denaturation[31]. The interaction of putrescine with α-Chy at different temperature conditions was evaluated by monitoring the intrinsic fluorescence intensity changes of α-Chy upon the addition of putrescine. α-Chy in solution was excited at 280 and 295 nm (excitation wavelength for Trp) and emission spectra were recorded in the

range of 290–450 nm (the emission maximum of 333 nm) at 25 and 35 °C in the presence and absence of various concentrations of putrescine, as shown in Fig. 6 and 7. Putrescine decreased α-Chy fluorescence intensity, but did not have any red or blue shift. The microenvironment around chromospheres (Trp) of α-Chy was changed. The change of α-Chy fluorescence at two temperatures was different. At the temperature of 35 ºC, under a similar concentration of putrescine, the emission maximum was higher and the emission maximum exhibited a larger decrease in the fluorescence intensity. The changes in fluorescence intensity were low, and remained around 0.4- 0.8 mM putrescine. After that, no significant changes were observed in all spectra recorded. Most of the Trp residues on α-Chy showed low accessibility to the solvent (residues 27, 29, 51, 141, 172 and 215), with less than 20% of their area exposed to the aqueous medium. Only two Trp residues presented around 46% (Trp207) and 49% (Trp237) of the exposed area to the solvent[35]. The changes in fluorescence intensity on α-Chy spectrum could be due to a local effect on these residues when binding to the putrescine without the occurrence of a conformational change. This indicated that the putrescine had interacted with α-Chy, thereby changing the structure of this protein, especially the microenvironment of Trp residues; this, in turn, led to a less hydrophobic environment for the fluorescence fluorophore placed. Fluorescence quenching spectra of α-Chy in the presence of various concentrations of putrescine are shown in figs. 6 and 7.

3.5. Mode of fluorescence quenching

Intrinsic fluorescence quenching may give elements some estimation of the binding mechanism of ligand to protein[41]. By measuring the intrinsic fluorescence quenching of α-Chy, the accessibility of the quenchers to the fluorophore groups of α-Chy can be estimated. This information can help us predict the binding mechanisms of putrescine to α-Chy. Fluorescence quenching proceeds via different mechanisms usually classified as dynamic

quenching, static quenching or static and dynamic quenching simultaneously. Dynamic quenching results from collisional encounters between the fluorophore and quencher, while the static one originates from the formation of a ground-state complex between the fluorophore and the quencher. In both cases, molecular contact is required between the fluorophore and the quencher for fluorescence quenching to occur[22, 42-44]. Quenching mechanism is described by the Stern–Volmer equation[45-47] (Eq. (5)):

$$\frac{F0}{F} = 1 + K_{sv}[Q] = 1 + K_q\tau_0[Q] \qquad \text{Eq. (5)}$$

, where F_0 and F are the fluorescence intensities of α-Chy in the absence and presence of putrescine (quencher), respectively; [Q] is the total concentration of the quencher (putrescine); and K_{SV} is the Stern–Volmer quenching constant, which is described by the following equation[48] (Eq. (6))

$$K_{sv} = k_q\tau_0 \qquad \text{Eq. (6)}$$

, where k_q is the quenching rate constant of the biological macromolecule and τ_0 is the fluorescence average lifetime of the fluorophore (in this case Trp), which has been reported for the Trp residues of α-Chy at the neutral pH as 2.96×10^{-9} s [22, 49]. Eq. 1 was applied to determine Ksv by the linear regression of a plot of F_0/F against the concentration of putrescine. F_0 and F are the steady state fluorescence intensities of α-Chy at 333 nm before and after the addition of quencher (putrescine), K_{sv} and [Q] are the Stern–Volmer dynamic quenching constant and the concentration of quencher putrescine, respectively, k_q is the quenching rate constant of biomolecule, and τ_0 is the average life-time of bimolecular without the quencher, with its value being 2.96 ns[9, 22, 49]. Quenching data are usually presented as plots of F_0/F versus [Q]. A plot of $F0/F$ versus [Q] yields an intercept of one on the y-axis and a slope equal to K_{SV}. As shown in Fig.8. Stern–Volmer plots were plotted based on Eq. (6). The solid lines in figure 8 show the lines of the best fit of the experimental data to the Stern–Volmer equation. A linear Stern- Volmer plot is generally indicative of a single class of fluorophores, all equally accessible to the quencher. If two fluorophore populations are

present, and one class is not accessible to the quencher, then the Stern-Volmer plots deviate from linearity toward the x-axis. This is frequently found for the quenching of tryptophan fluorescence in proteins by polar or charged quenchers. These molecules do not readily penetrate the hydrophobic interior of proteins, and only those tryptophan residues on the surface of the protein are quenched[43]. Static and dynamic quenching can be distinguished by their differing dependence on temperature and viscosity, or, preferably, by lifetime measurements. Higher temperatures result in faster diffusion and hence, larger amounts of collisional quenching. Higher temperatures will also typically result in the dissociation of weakly bound complexes and hence, smaller amounts of static quenching. The increase of K_{SV} with temperature indicated dynamic quenching**.** In Table 3, the binding constant was obtained from the Stern-Volmer method and listed for Putrescine with α-Chy. The K_q, the quenching rate constant, was less than 2.0×10^{10} L $mol^{-1}s^{-1}$. This also indicated that the quenching of α-Chy fluorescence by Putrescine was the dynamic one (Fig. 8).

3.6 Enzymatic Activity of α-Chymotrypsine

The enzymes structure and conformational dynamics are influenced by temperature. But too low or high temperatures denature proteins, thereby deactivating their function too. Moreover, cosolvents can stabilize or destabilize the conformation of proteins and therefore, influence their enzymatic activity. Polyamine analogues can prevents proteins against proteolysis and degradation. The stabilization of proteins from its normal rapid turnover appears to be due to a conformational change in the protein after the non-covalent binding of the polyamine or analogue that decreases the ability of protein to serve as a substrate for proteolysis[50]. A possibility to change the enzyme surface features, increasing the protein stability at a material interface, is to carry out chemical modification. Immobilization of enzymes and Polymer conjugation or the attachment of poly (ethylene glycol) or of small molecules as

carbohydrates and polyamines such as putrescine might alter the surface of an enzyme, providing additional points of hydrogen bonding on the enzyme surface, decreasing dehydration, or rendering the unfolding less thermodynamically favorable. Stabilization of monomeric enzymes via multipoint covalent attachment or generation of favorable environments surrounding the enzyme has been reported in many instances, while multimeric enzymes have been stabilized by immobilizing all enzyme subunits, thus preventing subunit dissociation[51-54].Addition of Putrescine to α-Chy solution stabilizes the enzyme by an increase in the unfolding temperature, Tm. To ascertain whether the Putrescine could cause any alternation in the enzyme activity of the folding transition state of α-Chy, we further performed enzyme activity experiments. We tested the α-Chy activity in the presence of Putrescine using UV-Vis spectrophotometer. The obtained results have been represented and displayed in Figure 9. The enzymatic activities of α-Chy in presence and absence of Putrescine were measured at 37 °C and the pH=8.0 (Figure 9, the double reciprocal plot of line weaver-Burk). It could be observed from Fig. 9 that the activity of α-Chy was increased with increasing the concentration of Putrescine. Under the concentration conditions used here, the enzyme kinetics of α-Chy could be described by the Michaelis–Menten kinetics:

$$E+S \underset{K^{-}1}{\overset{K_1}{\leftrightarrow}} ES \xrightarrow{K_2} E+P$$

,where k_1, k_{-1}, and k_2 are rate constants. The initial velocity of the enzyme reaction v_0 (v_0=d[p]/dt, where [P] is the concentration of the product), i.e., the rate of product formation, was calculated from the slope of the linear fit of the time dependent absorbance data at 256 nm. The kinetic parameters K_m= (K_{-1}+K_2)/K_1 (Michaelis constant) could be obtained by the linear regression analysis of the Lineweaver–Burk plot (Eq. (6)):

$$\frac{[E]}{V_0} = \frac{[E]}{V_{max}} + \frac{[E].K_m}{V_{max}} \times \frac{1}{[S]} = \frac{1}{K_{cat}} + \frac{K_m}{K_{cat}} \times \frac{1}{[S]} \qquad \text{Eq. (6)}$$

, where [E] is the total enzyme concentration, [S] is the initial substrate concentration, and V_{max} is the maximum achievable rate enzyme. As illustrated in Fig. 9, as the concentration of Putrescine was increased, the maximum rate of α-Chy (V_{max}) was increased too. Putrescine is a nonessential activator for α-Chy. What determines the activation characterization of a moderator are the values of α and β parameters. Both α and β parameters could be deduced from Eq. (7) [55,56]:

$$\frac{1}{V} = \frac{K_m}{V_{max}} \frac{1+\frac{A}{K}}{1+\frac{\beta[M]}{\alpha K}} \times \frac{1}{[S]} + \frac{1}{V_{max}} \frac{\beta-1}{\alpha-\beta} \qquad \text{Eq. (7)}$$

The activation of an enzyme could be achieved by increasing the affinity of the binding of the substrate to the enzyme (α < 1) and/or increasing the catalytic constant (k_p) value by β (k'_p = β k_p). The following Scheme is a general representation to evaluate the activation together.

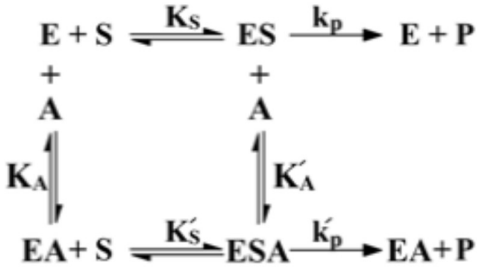

Reversible activation could be observed by the role of two α and β parameters. In the case of α = 1 and β > 1, the moderator activates the enzyme by increasing the catalytic constant (β > 1), without any effect on the affinity of the binding of the substrate to the enzyme (α = 1). This type of activator is not an essential activator because the enzymatic reaction is done without the activator. The Lineweaver-Burk plots in the absence and presence of a non-essential activator in different fixed concentrations intersect each other on the X-axis, implying that K_m does not change by the nonessential activator[56]. In our studies, with α = 1.001 and β= 3.427, K_a was 506. Changes in k_{cat} can generally be interpreted in terms of cosolute-induced variations of the catalytic rate constant and the effective enzyme concentration. The former effect may derive from minor conformational changes, hydration

changes, an increase of the dynamics in the enzyme active site (e.g., by breaking hydrogen bonds), or the destabilization of the enzyme–product complex[57].

3.7. Molecular Docking Studies

The results of docking could help to identify the potential localization of binding sites and show a unique site of interaction between α-Chy and Putrescine (Table4).Also, Fig.10 shows H-bond and hydrophobic analysis of docking poses by Ligplot plus tool for Putrescine ligands in α-Chy and Fig. 11 displays the interaction of Putrescine with the receptor α-Chy. The three-dimensional (3D) structure of α-Chy was obtained from the protein database, PDB. Autodock needed receptor and ligand representations in a file format called pdbqt, a modified protein data bank. For docking the Putrescine in to the binding site of the α-Chy, we used AutoDock 4.2 Software. The search algorithm was used in AutoGrid program based on defining all active molecules and generating the grid parameter files. Then, scoring algorithm in Autodock program was used for the binding conformation of ligand. By using Lamarckian genetic algorithm (LGA), hundred runs of docking were performed. Ligplot plus was used to analyze docking poses for Hydrogen bonding and hydrophobic bonding. A single binding site could be deduced from the analysis of spectroscopic studies. Since docking results could indicate changes occurring in the α-Chy structure during binding of Putrescine, they would mostly correspond to what was predicted by molecular modeling. As can be seen in $\Delta H^{\circ} < 0$ and $\Delta S^{\circ} > 0$ (Entropy, S = 9.15), the docking calculations suggested that a predominant contribution for binding came from hydrogen bonds interactions between Putrescine and α-Chy (Fig 10 and 11). The Gibbs free energy (ΔG^{o}) of Putrescine binding to α-Chy was equal to −6.11 kJ mol^{-1}, showing agreement with the experimental results. Nevertheless, the negative sign of ΔG^{o} corresponded well with the experimental results, thereby indicating that the binding process

was spontaneous. The theoretical distance between α-Chy and Putrescine, as calculated during docking studies, was 40.490 angstrom.

Molecular dynamic simulation (MD) Analysis:

The root mean square deviation (RMSD) was calculated for protein backbone using the starting structure (in the presence of Putrescine) as a reference obtained after 10 ns by MD simulation (Fig.12 and Table 5). The stability of the protein α-Chy during the simulation was evaluated by the RMSD of protein relative to the starting structure. As documented in Fig.12, the RMSD of protein in the presence of Putrescine was stable over time. This consistency indicated that the protein was stable under the simulation conditions. Variation in total energy versus time for 10 ns MD simulations was 0.0007 and the kinetics and potential energy fluctuated in equal and opposite direction for MD simulation, so the law of the conservation of energy in a system could be established during the simulation (Fig. 13). Table 5 shows protein backbone RMSD, radius of gyration (Rg), temperature, potential energy and secondary structure elements at the last 8 ns MD simulations for α-Chy: Putrescine in the presence of Na^+ and Cl^- ions. Average Rg at the last 8 ns MD simulations and low standard deviation indicated that the protein reached equilibrium during the simulation of structure.

4. Conclusion

This paper reported on a spectroscopic study, kinetic measurements, molecular dynamic simulations and molecular docking effects on the interaction of α-Chy as a model protein with putrescine. The experimental results indicated that the microenvironments of the tryptophan residue of α-Chy were changed by putrescine and also, the quenching mechanism of α-Chy by Putrescine was a dynamic quenching procedure. Molecular dynamic simulations demonstrated that Putrescine acted as a stabilizer at these concentrations. Kinetics results and

thermal studies also demonstrated that by increasing the concentration of putrescine, the stability and activity of the enzyme were enhanced. The docking study also indicated that putrescine was especially absorbed on the surface of the enzyme, leading to the increase of the thermal stability.

Acknowledgement

The work was financially supported by Shahrekord University, Iran.

References

1. M. J. Moreau, I. Morin and P. M. Schaeffer, *Molecular BioSystems*, 2010, **6**, 1285-1292.
2. K. A. Dill, *Biochemistry*, 1990, **29**, 7133-7155.
3. A. Kumar, P. Attri and P. Venkatesu, *Thermochimica Acta*, 2012, **536**, 55-62.
4. N. Rezaei-Ghaleh, A. Ebrahim-Habibi, A. A. Moosavi-Movahedi and M. Nemat-Gorgani, *International journal of biological macromolecules*, 2007, **41**, 597-604.
5. K. Igarashi and K. Kashiwagi, *IUBMB life*, 2015.
6. M. Vuento, E. Salonen and P. Riepponen, *Biochimie*, 1980, **62**, 99-104.
7. A. J. Geall, M. A. Eaton, T. Baker, C. Catterall and I. S. Blagbrough, *FEBS letters*, 1999, **459**, 337-342.
8. A. M. Klibanov, *Nature*, 2001, **409**, 241-246.
9. J. Tian, S. Wei, Y. Zhao, R. Liu and S. Zhao, *Journal of chemical sciences*, 2010, **122**, 391-400.
10. P. M. Reddy, R. Umapathi and P. Venkatesu, *Physical Chemistry Chemical Physics*, 2015, **17**, 184-190.
11. H. T. Wright, *Journal of molecular biology*, 1973, **79**, 1-11.
12. G. M. Morris, R. Huey, W. Lindstrom, M. F. Sanner, R. K. Belew, D. S. Goodsell and A. J. Olson, *Journal of computational chemistry*, 2009, **30**, 2785-2791.
13. P. W. Rose, A. Prlić, C. Bi, W. F. Bluhm, C. H. Christie, S. Dutta, R. K. Green, D. S. Goodsell, J. D. Westbrook and J. Woo, *Nucleic acids research*, 2015, **43**, D345-D356.
14. M. Frisch, G. Trucks, H. Schlegel, G. Scuseria, M. Robb, J. Cheeseman, J. Montgomery, T. Vreven, K. Kudin and J. Burant, 2008.
15. E. Project, E. Nachliel and M. Gutman, *Journal of computational chemistry*, 2010, **31**, 1864-1872.
16. W. F. van Gunsteren, S. Billeter, A. Eising, P. H. Hünenberger, P. Krüger, A. E. Mark, W. Scott and I. G. Tironi, 1996.
17. T. Darden, D. York and L. Pedersen, *The Journal of chemical physics*, 1993, **98**, 10089-10092.
18. B. Hess, H. Bekker, H. J. Berendsen and J. G. Fraaije, *Journal of computational chemistry*, 1997, **18**, 1463-1472.
19. S. Miyamoto and P. A. Kollman, *Journal of computational chemistry*, 1992, **13**, 952-962.
20. H. J. Berendsen, J. P. M. Postma, W. F. van Gunsteren, A. DiNola and J. Haak, *The Journal of chemical physics*, 1984, **81**, 3684-3690.
21. Q. Yang, J. Liang and H. Han, *The Journal of Physical Chemistry B*, 2009, **113**, 10454-10458.

22. Y. Liu and R. Liu, *Food and Chemical Toxicology*, 2012, **50**, 3298-3305.
23. Z. Chi, R. Liu, Y. Teng, X. Fang and C. Gao, *Journal of agricultural and food chemistry*, 2010, **58**, 10262-10269.
24. Z. Chi, R. Liu and H. Zhang, *Biomacromolecules*, 2010, **11**, 2454-2459.
25. A. Saboury and A. Moosavi-Movahedi, *Biochemical education*, 1995, **23**, 164-167.
26. A. Saboury and F. Karbassi, *Thermochimica acta*, 2000, **362**, 121-129.
27. P. Venkatesu, M.-J. Lee and H.-m. Lin, *The Journal of Physical Chemistry B*, 2007, **111**, 9045-9056.
28. H. N. Ong, B. Arumugam and S. Tayyab, *Journal of biochemistry*, 2009, **146**, 895-904.
29. A. A. A. Halim, H. A. Kadir and S. Tayyab, *Journal of biochemistry*, 2008, **144**, 33-38.
30. A. Kumar and P. Venkatesu, *Chemical reviews*, 2012, **112**, 4283-4307.
31. A. Kumar, A. Rani and P. Venkatesu, *New Journal of Chemistry*, 2015, **39**, 938-952.
32. V. Z. Pletnev, T. S. Zamolodchikova, W. A. Pangborn and W. L. Duax, *Proteins: Structure, Function, and Bioinformatics*, 2000, **41**, 8-16.
33. N. Wang, L. Ye, F. Yan and R. Xu, *International journal of pharmaceutics*, 2008, **351**, 55-60.
34. R. W. Woody and A. K. Dunker, in *Circular dichroism and the conformational analysis of biomolecules*, Springer, 1996, pp. 109-157.
35. M. Celej, M. D'andrea, P. Campana, G. Fidelio and M. BIANCONI, *Biochem. J*, 2004, **378**, 1059-1066.
36. X. Liu, L. Shang, X. Jiang, S. Dong and E. Wang, *Biophysical chemistry*, 2006, **121**, 218-223.
37. B. Ghalandari, A. Divsalar, M. Eslami-Moghadam, A. A. Saboury, T. Haertlé, M. Amanlou and K. Parivar, *Applied biochemistry and biotechnology*, 2015, **175**, 974-987.
38. T. De Diego, P. Lozano, S. Gmouh, M. Vaultier and J. L. Iborra, *Biotechnology and bioengineering*, 2004, **88**, 916-924.
39. A. Tulinsky and R. A. Blevins, *Journal of Biological Chemistry*, 1987, **262**, 7737-7743.
40. A. Sułkowska, *Journal of molecular structure*, 2002, **614**, 227-232.
41. Y. Yue, X. Chen, J. Qin and X. Yao, *Colloids and Surfaces B: Biointerfaces*, 2009, **69**, 51-57.
42. B. Pan, Y. Liu, D. Xiao, F. Wu, M. Wu, D. Zhang and B. Xing, *Environmental Pollution*, 2012, **161**, 192-198.
43. J. R. Lakowicz, *Principles of fluorescence spectroscopy*, Springer Science & Business Media, 2013.
44. A. Papadopoulou, R. J. Green and R. A. Frazier, *Journal of agricultural and food chemistry*, 2005, **53**, 158-163.
45. M.-F. Zhang, Z.-Q. Xu, Y.-S. Ge, F.-L. Jiang and Y. Liu, *Journal of Photochemistry and Photobiology B: Biology*, 2012, **108**, 34-43.
46. J. R. Lakowicz and G. Weber, *Biochemistry*, 1973, **12**, 4161-4170.
47. J. Min, X. Meng-Xia, Z. Dong, L. Yuan, L. Xiao-Yu and C. Xing, *Journal of Molecular Structure*, 2004, **692**, 71-80.
48. S. Tabassum, W. M. Al-Asbahy, M. Afzal and F. Arjmand, *Journal of Photochemistry and Photobiology B: Biology*, 2012, **114**, 132-139.
49. M.-X. Xie, M. Long, Y. Liu, C. Qin and Y.-D. Wang, *Biochimica et Biophysica Acta (BBA)-General Subjects*, 2006, **1760**, 1184-1191.

50. C. S. COLEMAN, *Biochemical Journal*, 2001, **358**, 137-145.
51. A. S. Bommarius and M. F. Paye, *Chemical Society Reviews*, 2013, **42**, 6534-6565.
52. A. Liese and L. Hilterhaus, *Chemical Society Reviews*, 2013, **42**, 6236-6249.
53. R. C. Rodrigues, C. Ortiz, A. Berenguer-Murcia, R. Torres and R. Fernández-Lafuente, *Chemical Society Reviews*, 2013, **42**, 6290-6307.
54. F. Secundo, *Chemical Society Reviews*, 2013, **42**, 6250-6261.
55. I. H. Segel, *Enzyme kinetics*, Wiley, New York, 1975.
56. A. Saboury, *Journal of the Iranian Chemical Society*, 2009, **6**, 219-229.
57. T. Q. Luong and R. Winter, *Physical Chemistry Chemical Physics*, 2015, **17**, 23273-23278.

Legends for figures:

Fig. 1(a): UV–vis spectra of α-Chy in the presence and absence of putrescine (0-0.6 mM) at the of pH 8.0 and 298 K, and (b): absorbance at 280 nm in the presence and absence of putrescine(0-0.6 mM).

Fig.2. The fraction unfolded of α-Chy in various concentrations of Putrescine at the pH of 8.0.

Fig.3. The effect of putrescine on ΔG° of α-Chy in different concentrations of putrescine at the pH= 8.0.

Fig.4. Far-UV CD spectra of α-Chy in the presence and absence of putrescine at the pH of 8.0. The Y-axis is the mean-residue ellipticity with the unit of degree cm^2 $dmol^{-1}$.

Fig.5. Near-UV CD spectra of α-Chy in the presence and absence of putrescine at the pH of 8.0. The Y-axis is the mean-residue ellipticity with the unit of degree cm^2 $dmol^{-1}$.

Fig.6. a) Fluorescence quenching of α-Chy, λ_{exi}=280 nm**,** and λ_{emi}=290-450 in the presence of different concentrations of putrescine at the pH of 8.0 and 298 K, and b) Fluorescence intensity in 333 nm and in the presence of different concentrations of putrescine at the pH of 8.0 and 298 K.

Fig.7.a) Fluorescence quenching of α-Chy, λ_{exi}=280 nm**,** and λ_{emi}=290-450 in the presence of different concentrations of putrescine at the pH of 8.0 and 308 K, and b) Fluorescence intensity in 333 nm and in the presence of different concentrations of putrescine at the pH= 8.0 and 308 K.

Fig.8. Stern–Volmer plots for the quenching of α-Chy by putrescine at 25 and 35ºC, λ_{exi}=280 nm, λ_{emi}=290-450 nm, and the pH=8.0.

Fig.9. Line Weaver-Burk plot of α-Chy at various Putrescine concentrations (mM) at 37ºC, and the pH=8.0.

Fig.10. H-bond and hydrophobic analysis of docking poses by Ligplot plus tool for Putrescine ligands in α-Chy.

Fig.11. The interaction of Putrescine with the receptor α-Chy.

Fig.12 The root mean square deviation (RMSD) of protein backbone during 10 ns MD simulation.

Fig.13 The kinetics and potential energies in 10 ns MD simulation

Table 1: T_m changes of α-Chy at variable concentrations of putrescine

Concentration (mM)	T_m(K)
0.0	315
0. 1	324
0.2	323.6
0.3	323.6
0.7	322.6
1.0	320
2.0	320.6
3.0	319
4.0	320
5.0	320
10	321

Table 2: Content of the secondary structure of the α-Chy at the temperature of 25 ºC and the pH= 8.0

putrescine concentration (mmol L^{-1})	Content(%)			
	α-Helix(%)	β-Sheet(%)	β-Turn(%)	Random coil (%)
0	11.6	20.5	27.7	40.2
0.1	13.1	25.5	25	36.4
0.3	10	32	23	35

Table 3: Stern–Volmer quenching constants of the complex of α-Chy with putrescine at the pH= 8.

T(K)	K_{SV} (L mol^{-1})	k_q (L mol^{-1} S^{-1})	R^2
308	7.0×10^{-2}	24×10^{7}	0.9966
298	2.4×10^{-2}	81×10^{7}	0.9886

Table4: Docked Results with interacting residues after 100 runs of docking.

E_b (kcal/mol)	Final Intermolecular energy (kcal/mol)	Hydrogen Bond (kcal/mol)	Total Internal energy (kcal/mol)	Interaction bonds	
				Hydrogen-Bonding	Hydrophobic-Bonding
-6.11	-7.43	-2.13	0.74	Ala243, Asn245	-

Table 5: The average of RMSD, Rg, kinetic, Temperature, Number Hydrogen Bonds and potential energy during the last 8 ns of 10 ns MD simulation of protein α-Chy in presences of Putrescine.

Average Rg (nm)	Average RMSD (nm)	Average Potential (KJ/mol)	Average Total energy (KJ/mol)	Average Temperature (K)	Number Hydrogen Bonds	Drift ^{1} 10^{-4}
2.28±0.01	0.25±0.02	-746865±919	-611589±1322	299±1.4	854±0.32	7

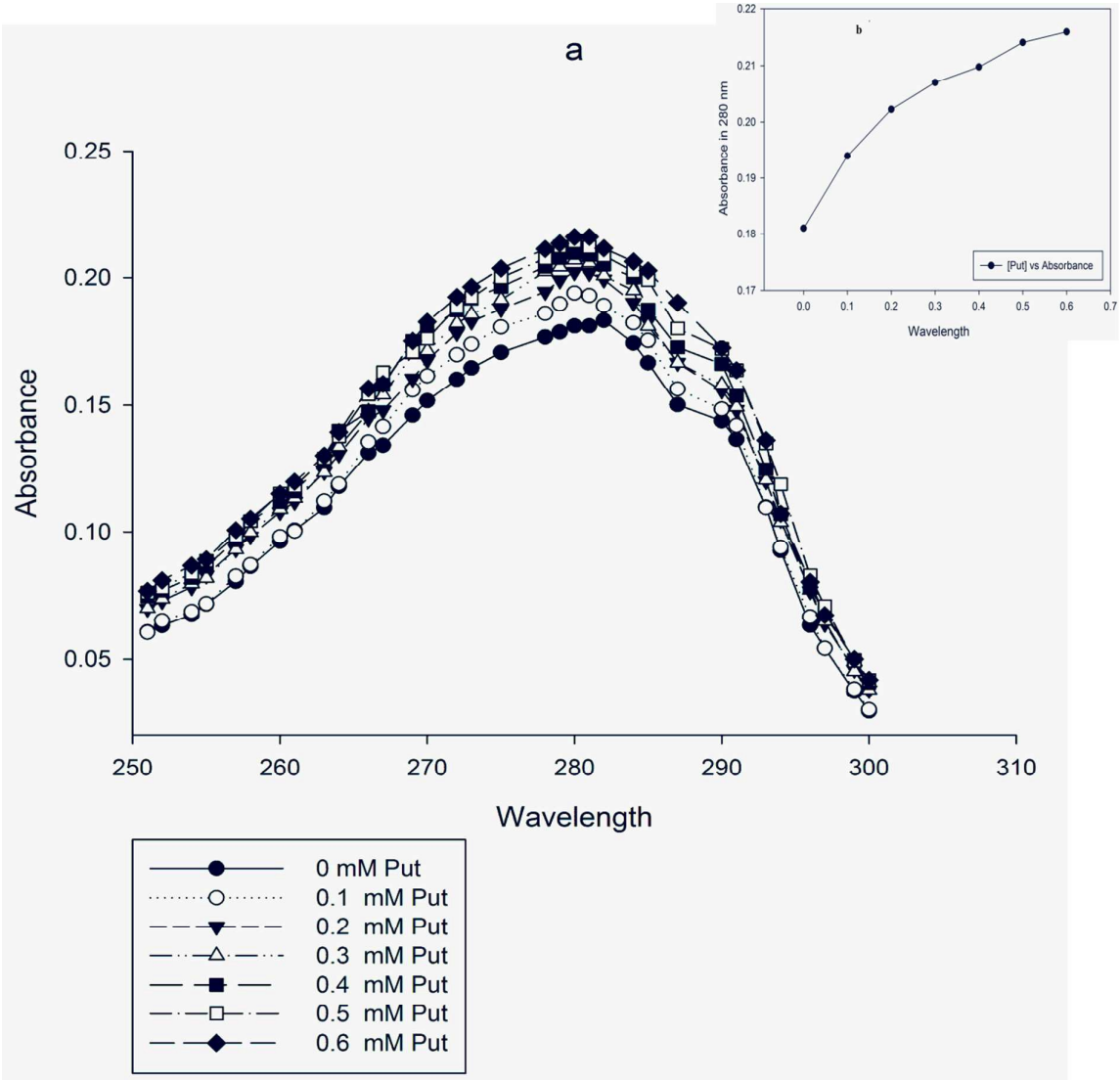

Fig. 1

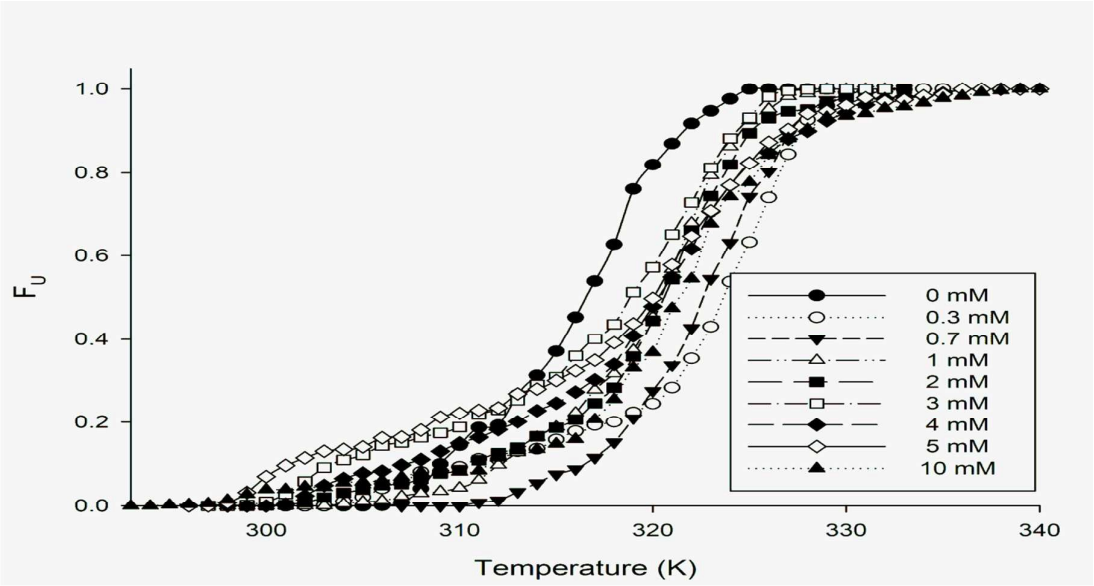

Fig. 2

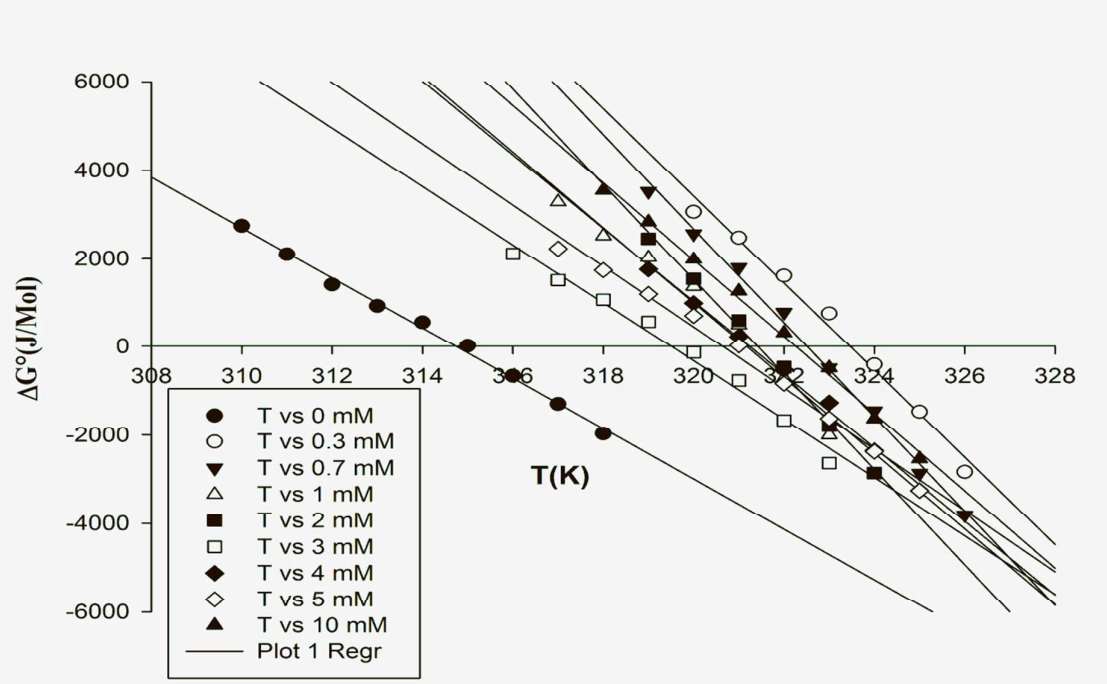

Fig. 3

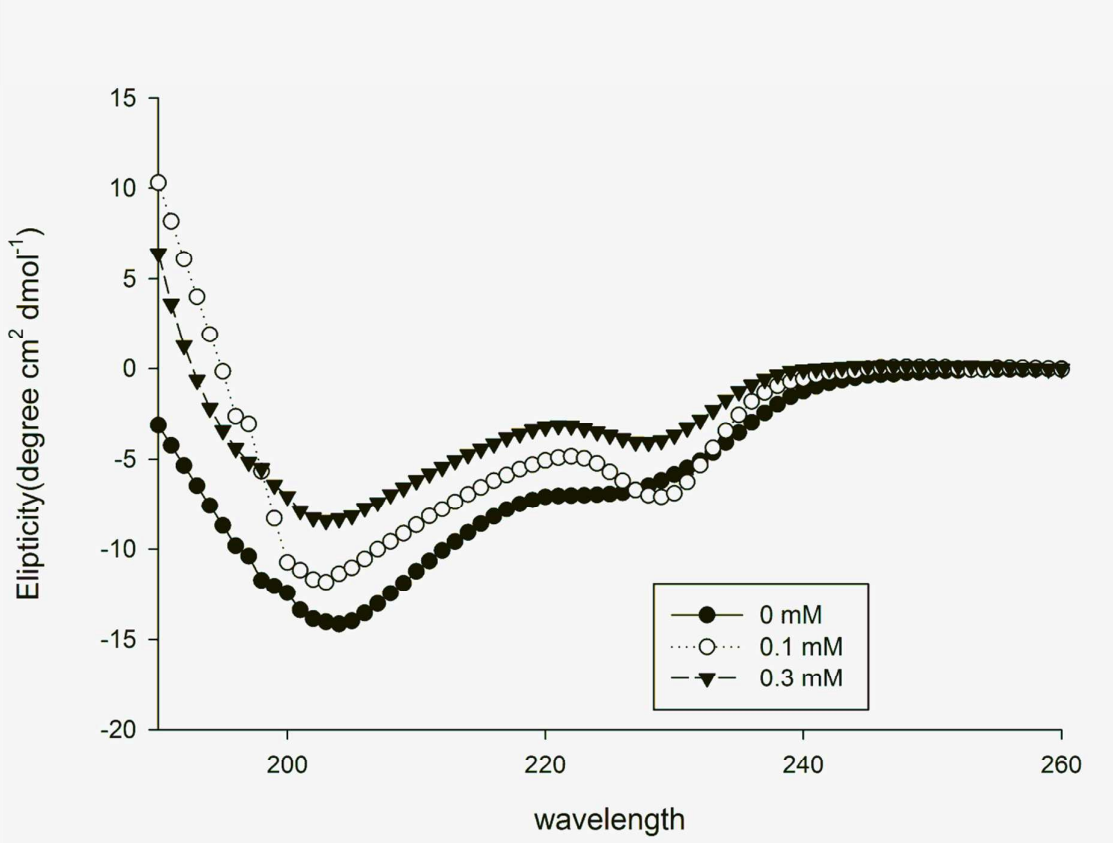

Fig.4

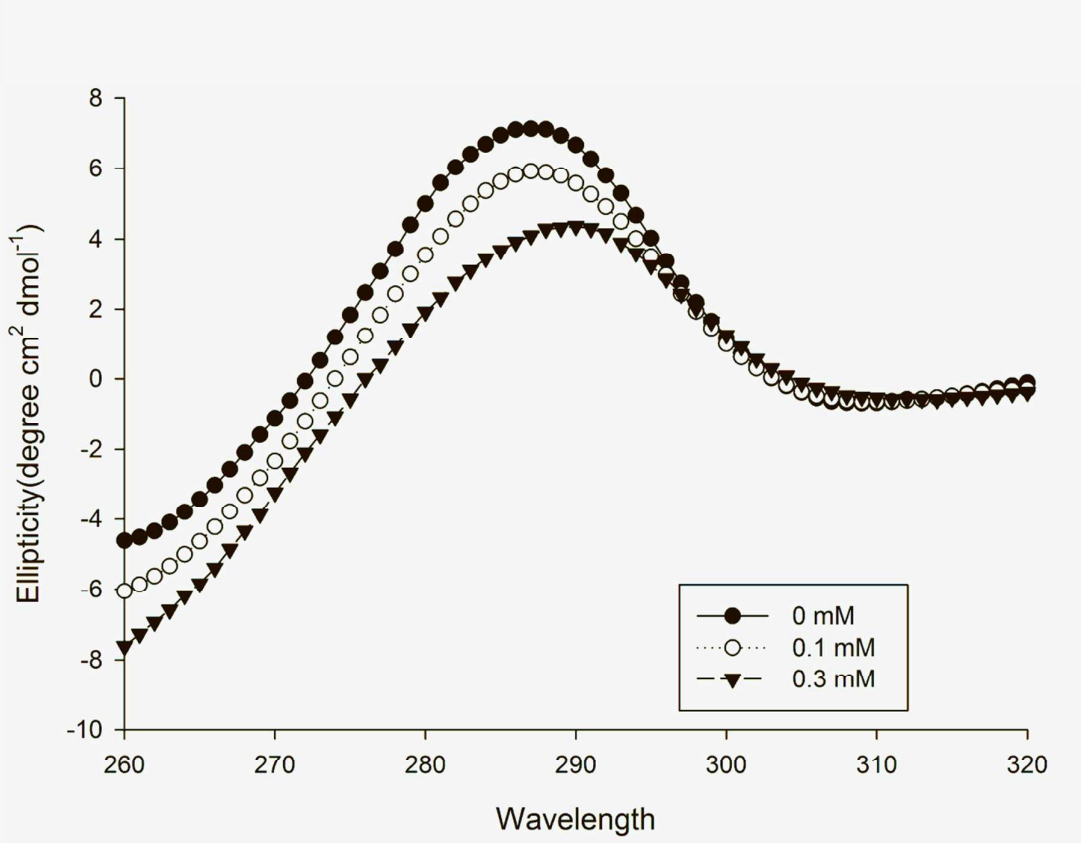

Fig. 5

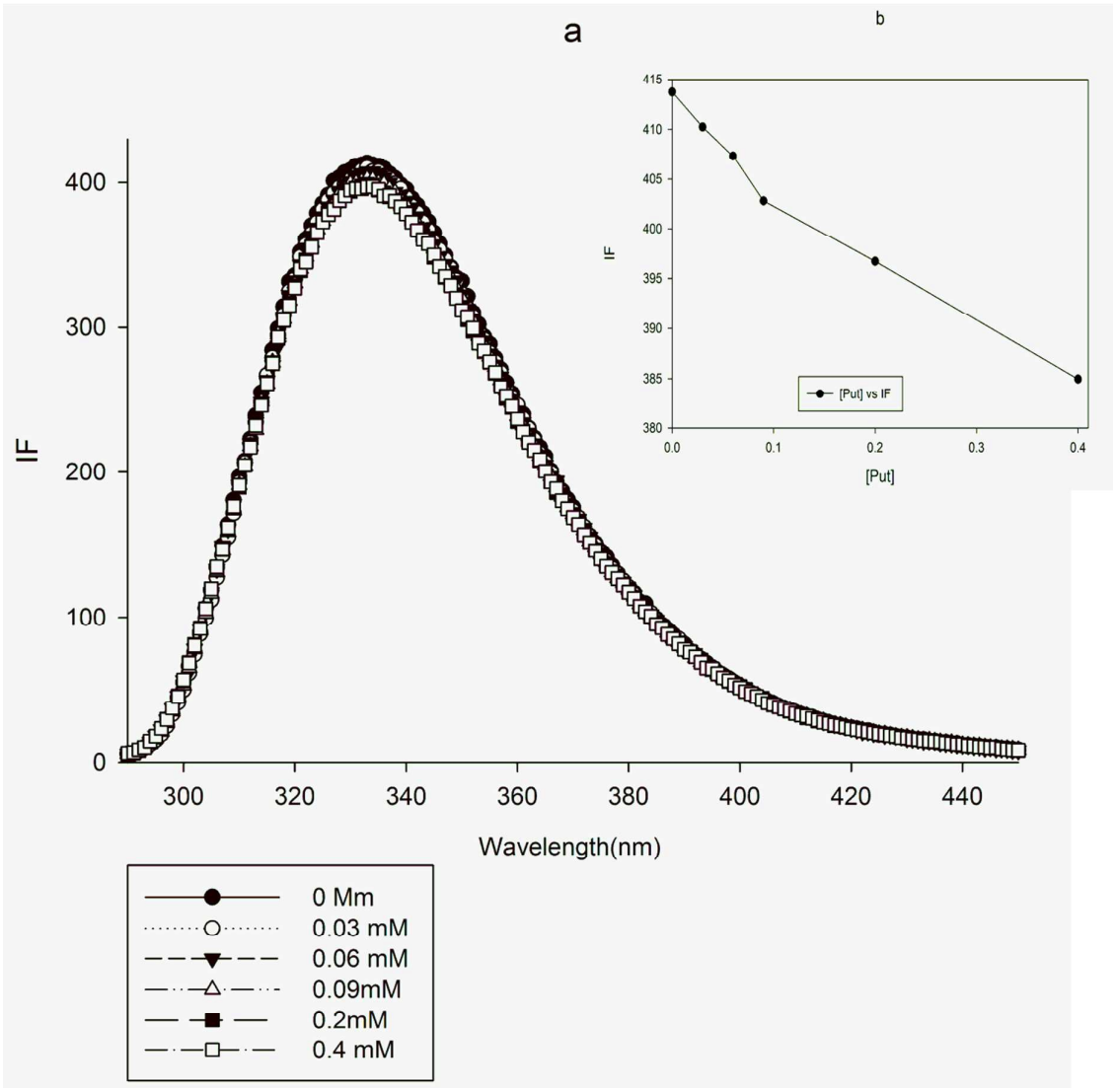

Fig. 6

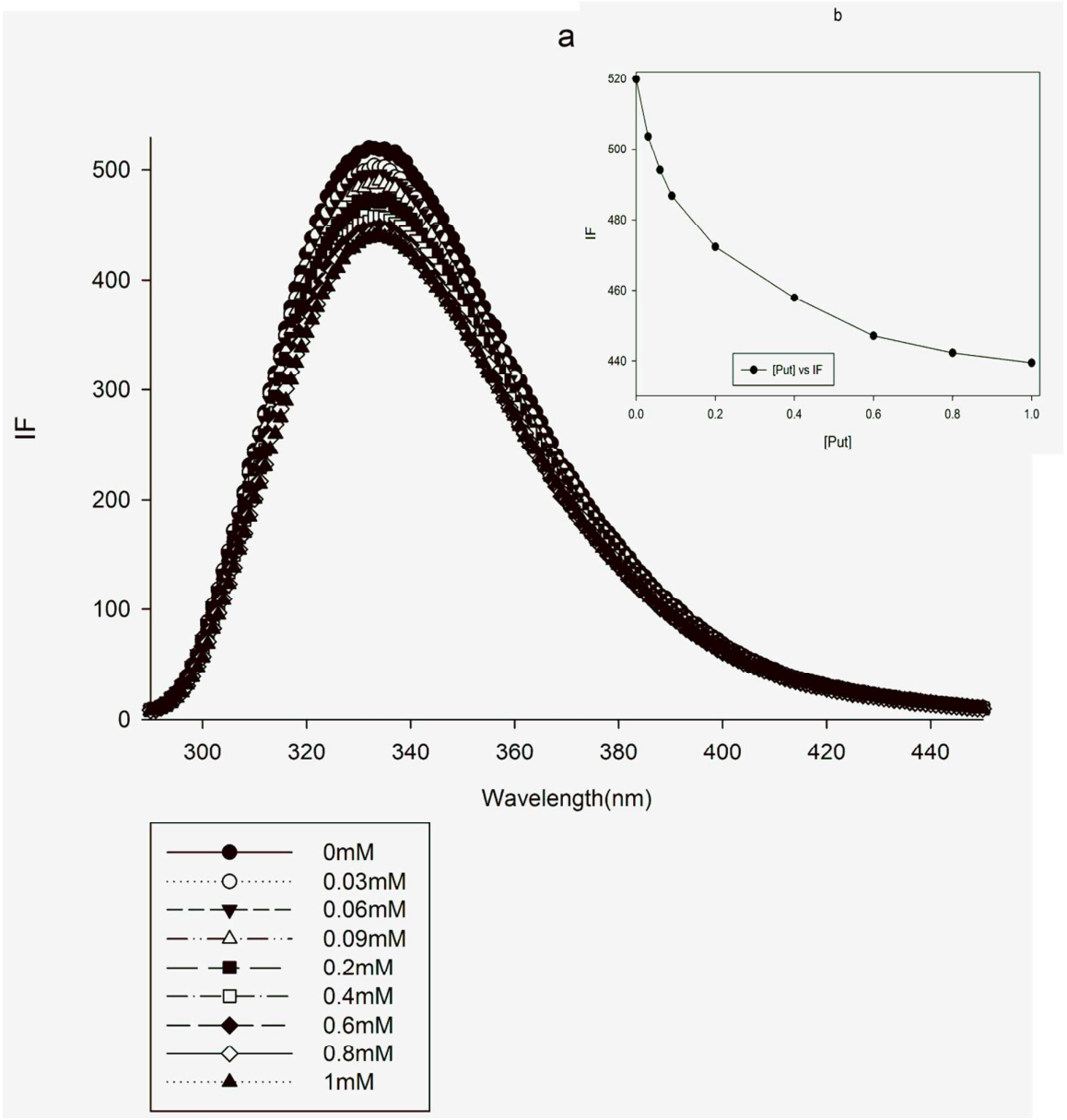

Fig. 7

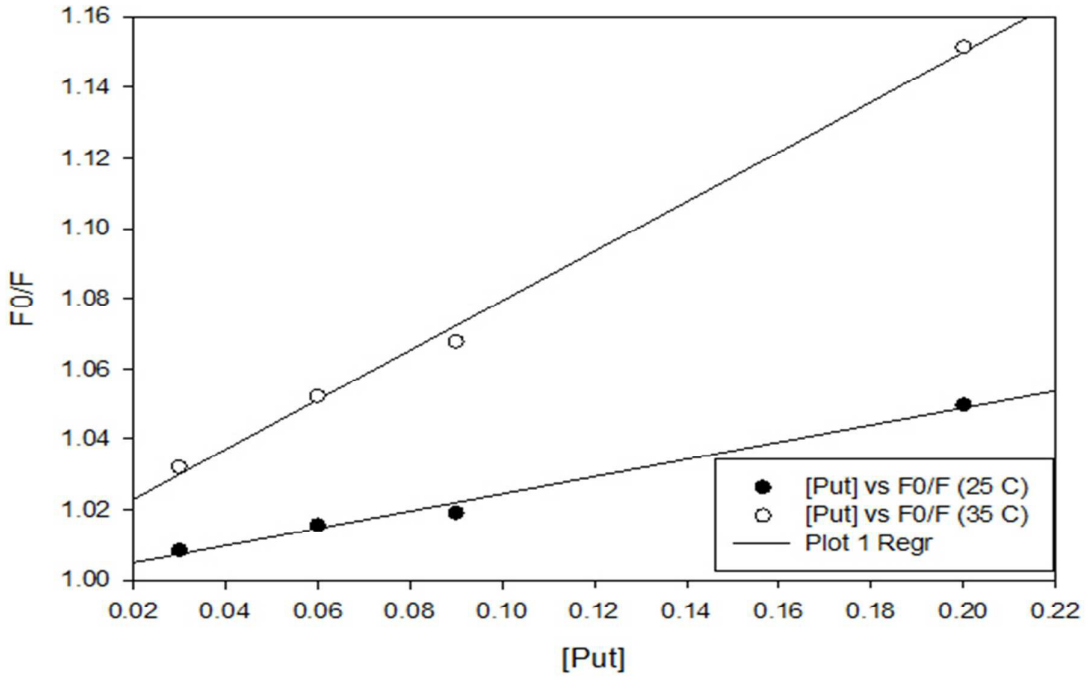

Fig. 8

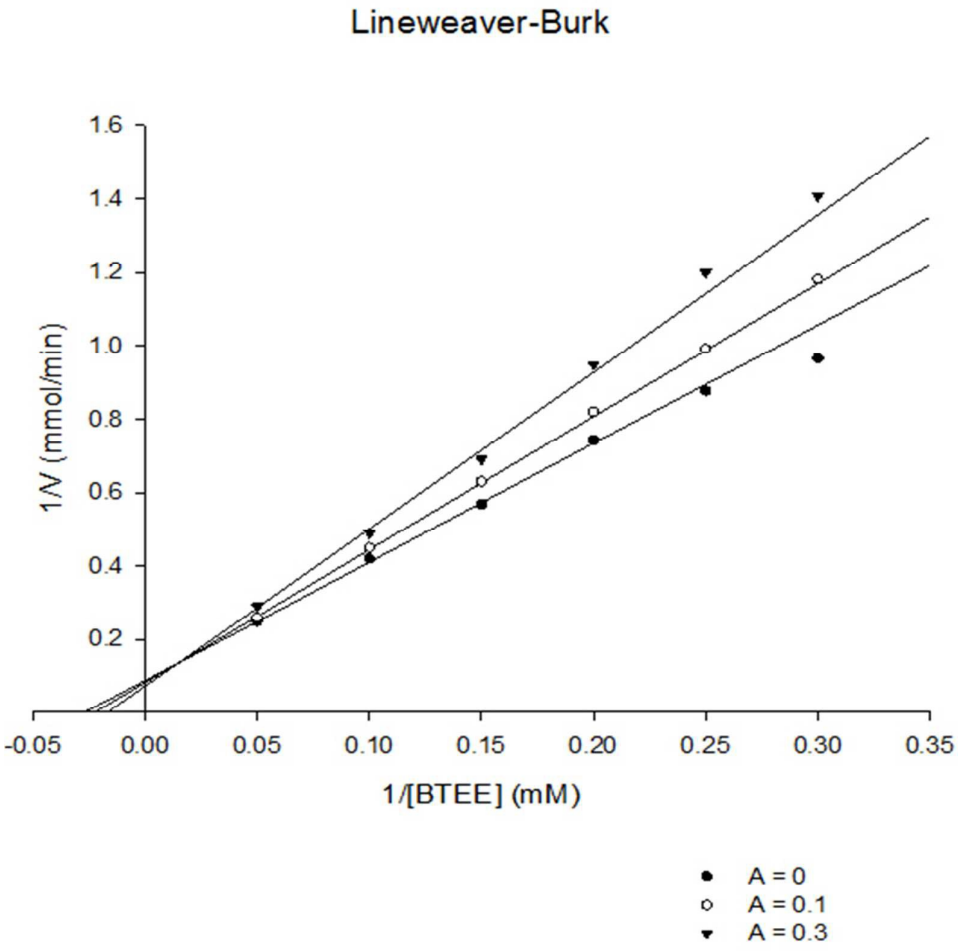

Fig. 9

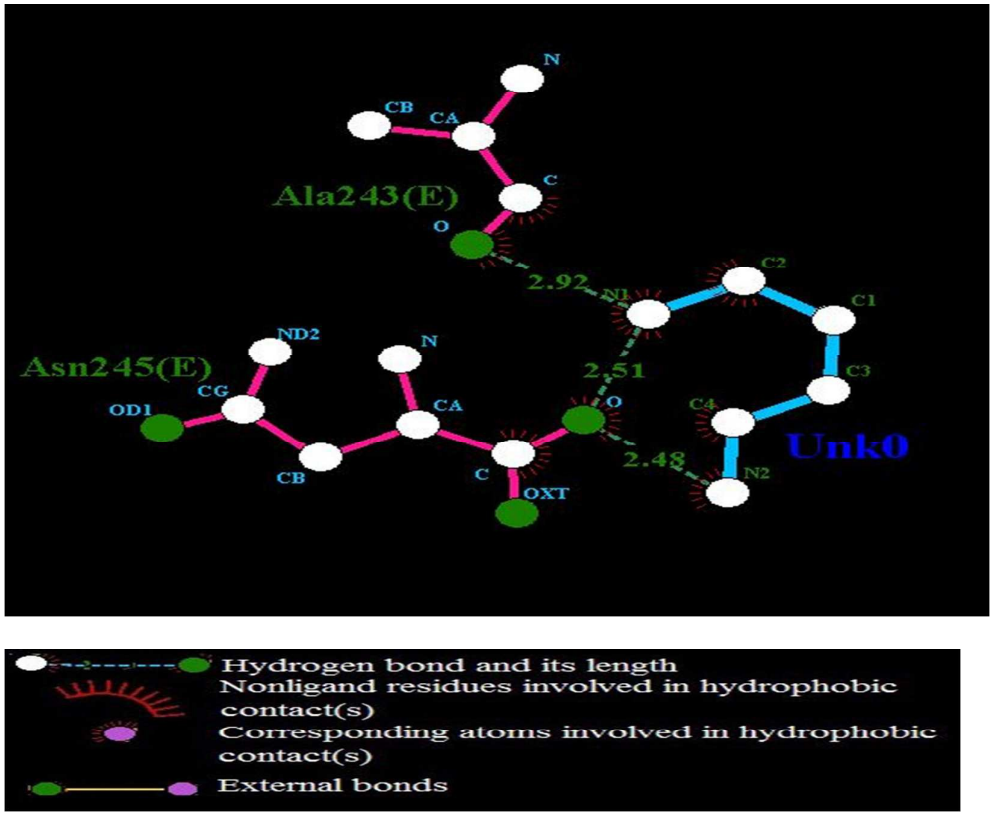

Fig. 10

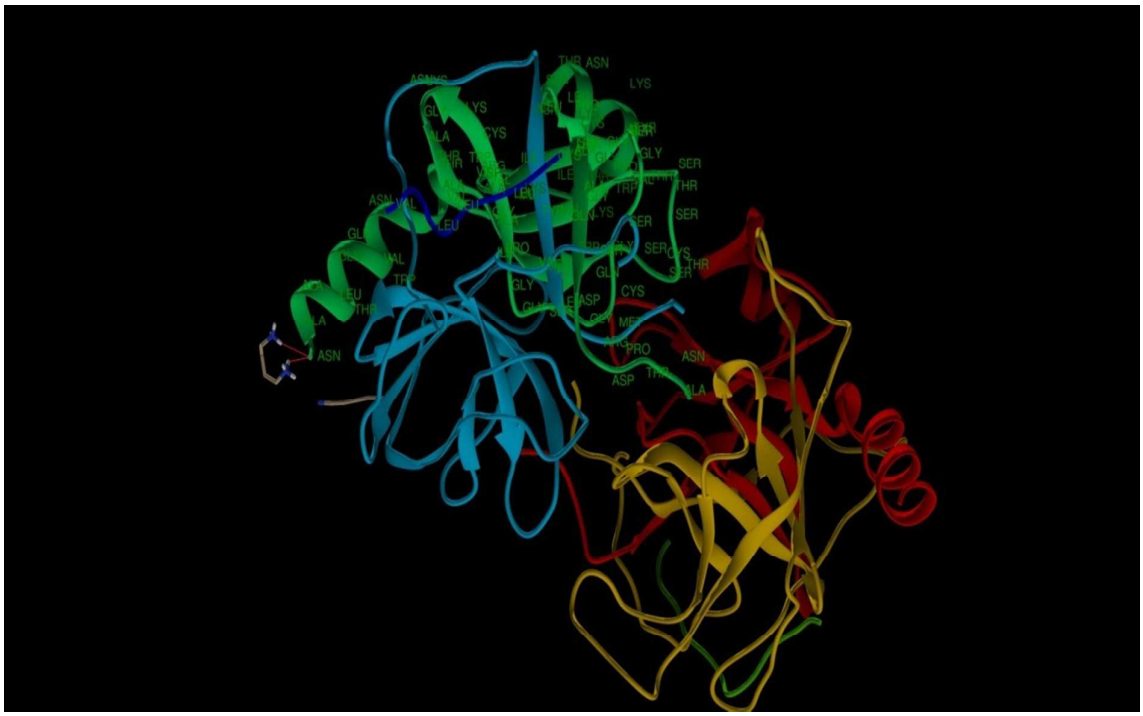

Fig. 11

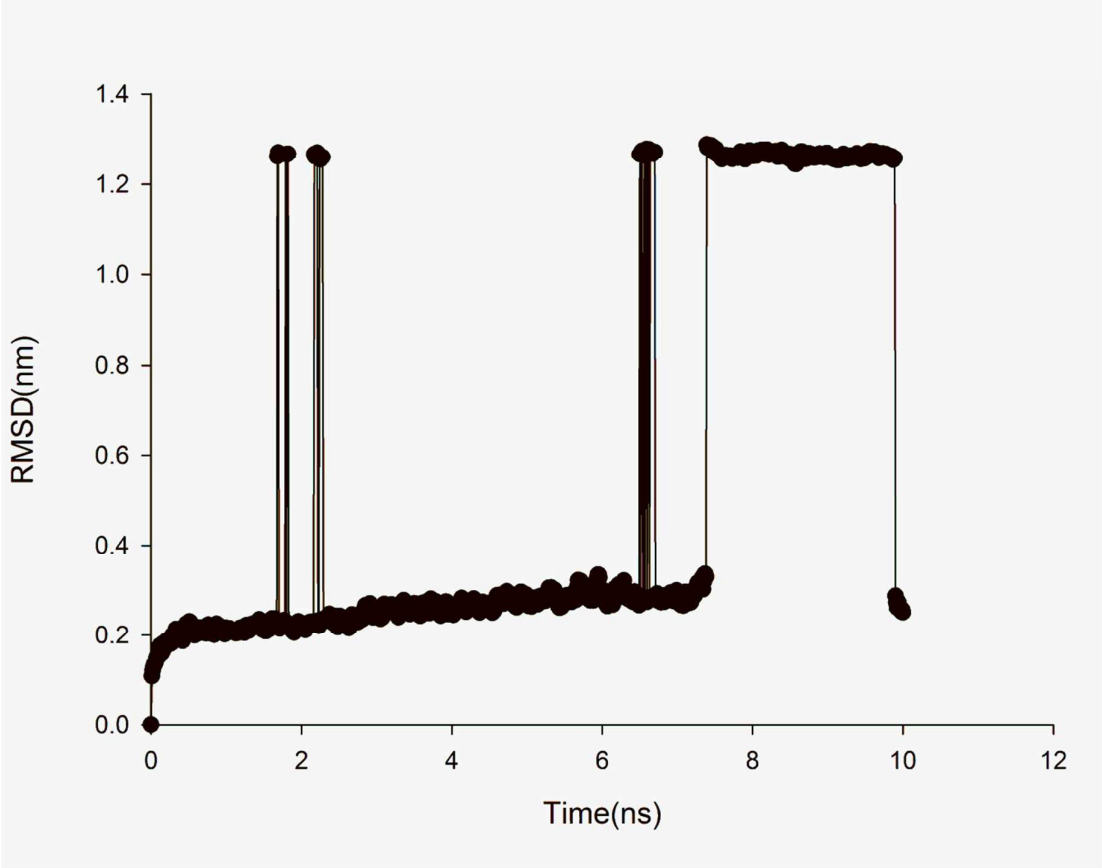

Fig. 12

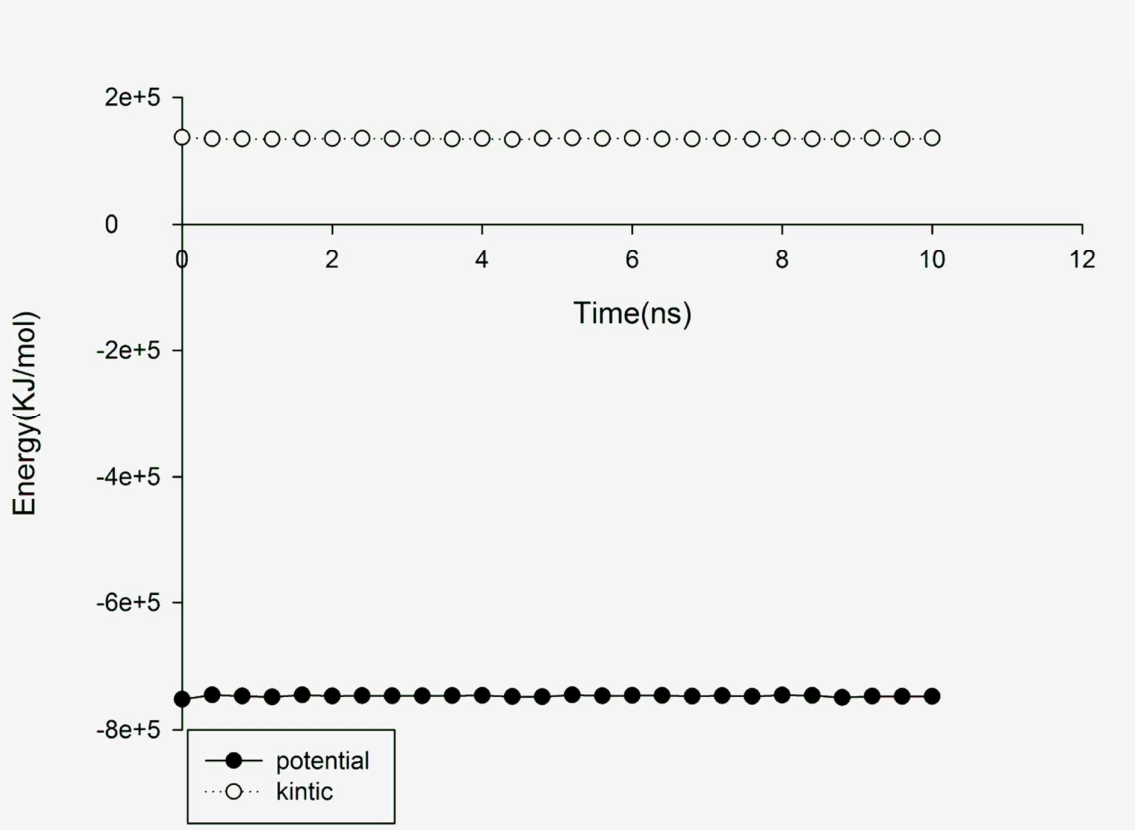

Fig. 13

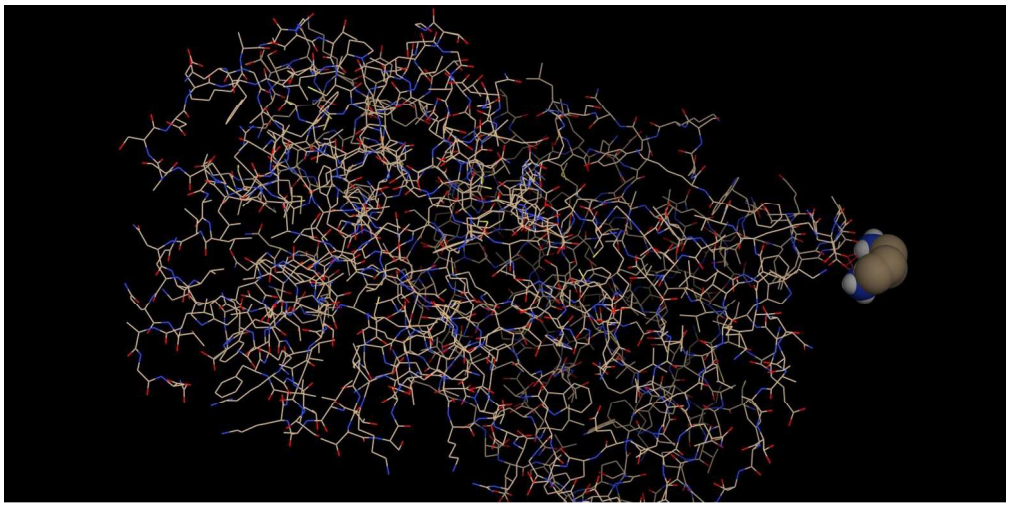

564x280mm (72 x 72 DPI)